IEEE Access
Multidisciplinary | Rapid Review | Open Access Journal

Received May 8, 2020, accepted May 19, 2020, date of publication May 25, 2020, date of current version June 8, 2020.

Digital Object Identifier 10.1109/ACCESS.2020.2997396

Joint Optimization of Survivability and Energy Efficiency in 5G C-RAN With mm-Wave Based RRH

BO TIAN[1,2,3], QI ZHANG[1,2], YIQIANG LI[1,2], AND MASSIMO TORNATORE[3], (Senior Member, IEEE)

[1]School of Electronic Engineering, Beijing University of Posts and Telecommunication, Beijing 100876, China
[2]Beijing Key Laboratory of Space-Round Interconnection and Convergence, Beijing 100876, China
[3]Department of Electronics, Information and Bioengineering, Politecnico di Milano, 20133 Milano, Italy

Corresponding author: Qi Zhang (zhangqi@bupt.edu.cn)

This work was supported in part by the National Key Research and Development Program of China under Grant 2018YFB1801302, in part by the National Natural Science Foundation of China (NSFC) under Grant 61675033 and Grant 61835002, and in part by the BUPT Excellent Ph.D. Students Foundation under Grant CX2019304.

ABSTRACT Centralized Radio Access Networks (C-RAN) exploiting millimeter wave (mm-wave) technology in remote radio heads (RRHs) are regarded as a promising approach to satisfy the challenging service requirements of fifth generation (5G) mobile communication. However, ultra-dense deployment of mm-wave RRHs will generate enormous amount of traffic that will require effective design and operation of C-RAN backhaul. In this paper, we focus on developing an optimal mm-wave RRHs placement strategy that exploits resource and traffic assignment in RRHs to achieve reliable and energy efficient backhaul transmissions. Specifically, in this paper, mm-wave is considered both to provide end users access and to interconnect RRHs in same frequency band, hence achieving energy saving thanks to hardware and frequency reuse. In this scenario, leveraging the traffic predictions obtained by a deep neural network, we present a real-time traffic assignment scheme where traffic from affected RRHs can be rerouted to other RRHs to protect against backhaul failures and traffic migrates to as few RRHs as possible to switch off some backhaul links for energy efficiency. Due to the inherent short-range transmission of mm-wave, different RRH deployment locations significantly affect interconnections in RRHs. Therefore, we model the mm-wave RRH placement problem into an optimization framework that jointly maximizes backhaul survivability and energy efficiency, whilst subjects to constraints as network coverage and capacity. To guarantee scalability of the proposed scheme as network scale increases, a heuristic algorithm is also proposed. Numerical evaluations show that, with appropriate RRH placement strategies, significant survivability and energy efficiency improvements can be achieved.

INDEX TERMS Centralized radio access network, backhaul link, millimeter wave, survivability, energy efficiency.

I. INTRODUCTION

The continuous growth in mobile broadband service and the emergence of new machine-centric applications are creating unprecedented network requirements that exceed the capabilities of current mobile network architecture [1], [2]. To accommodate these new network requirements, the development of the fifth generation (5G) cellular communication is currently underway. Centralized Radio Access Networks (C-RAN) has been recognized as a promising architecture to support high capacity, low latency and energy efficient communication in 5G [3], [4]. It separates the traditional base station (BS) into three parts, namely, the baseband unit (BBU) pool, remote radio heads (RRHs) and the high-bandwidth (typically, fiber-based) transport link connecting RRHs to the BBU pool. In C-RAN, most baseband signal processing tasks are moved to the BBU pool to enable centralized baseband signal processing, such that significant performance gain can be achieved in terms of increased resource utilization, lower energy consumption [5]. In particular, traffic prediction is

The associate editor coordinating the review of this manuscript and approving it for publication was Javed Iqbal.

an important phase to perform centralized resource planning, which enables collaborative transmission and real-time demand allocation [6]–[8]. For example, Ref. [6] proposes a deep-learning based traffic prediction for resource allocation in an intra-data-center network, while Recurrent Neural Networks are applied to predict baseband unit (BBU) pool traffic [7]. Traffic prediction is also an effective tool to carry out virtual topology reconfiguration [8].

A prominent feature of 5G is the deployment of ultra-dense small cells, exploiting wireless carrier in very high frequencies, such as millimeter wave (mm-wave), to extend transmission bandwidth [9]. Initial theoretical results on coverage and capacity of mm-wave based cellular networks show that coverage in mm-wave systems can rival or even exceed coverage in microwave systems assuming that the link budgets promised by existing mm-wave system designs are in fact achieved [10]. Other prototype test results showed that some mm-wave frequencies, e.g., 28GHz and 38GHz, can be used for 5G cellular networks employing steerable directional antennas, which demonstrates that mm-wave is capable of supporting a few-hundred-meter radius of outdoor and indoor coverage with more than 500Mb/s data rate [11], [12]. The key technology on mm-wave communication is beamforming-enabled massive Multiple-Input Multiple-Output (mMIMO), where each small cell is equipped with a large number of antennas and can serve multiple users over the same frequency and time band [13].

The deployment of small cells exploiting mm-wave in 5G can sustain the exponentially-growing traffic demand, but it also imposes extremely high requirements for backhaul[1] transmission [14]. As a result, different types of point to multipoint (PtMP) passive optical networks (PON), including variations of wavelength division multiplexing (WDM) PONs (e.g., coarse WDM (CWDM) PON, dense WDM (DWDM) PON), and Time WDM (TWDM) PON are investigated as effective backhaul solutions. In this study, we consider each mm-wave RRH can be assigned a unique optical wavelength to achieve ''any RRH-to-any BBU'' connection pattern without impact on latency [15], [16]. However, as users are typically not uniformly distributed, some backhauls of mm-wave RRHs may still suffer from heavy load, while their adjacent RRHs may carry only light load. Besides, as users move among different areas (e.g., residential, offices, and shopping malls) during a day, peak data requirements may vary as much as 10 times over time. To ensure robust data transmission at any time and any place, both the backhaul transport links and mm-wave processing capacity in RRHs are designed for peak data rate. As a result, the backhaul transmission resource and mm-wave resource are largely wasted, because most of the time these mm-wave RRHs are not working in full rate. Motivated by these inherent inefficiencies in mm-wave RRHs deployment, we provide an optimization scheme that achieves energy-efficient backhaul transmission in C-RAN.

Moreover, in C-RAN with mm-wave RRHs, if a backhaul fiber/component failure occurs, a large number of end users will be affected. For this reason, providing a reliable backhaul is extremely important. However, deploying redundant resources (i.e., optical fibers and optical switches) to protect against backhaul failures will bring significant cost overhead. Hence, in this work, we also aim at providing backhaul survivability while ensuring energy efficiency.

A. PRIOR WORK

Survivability of integrated fiber-wireless networks has been subject of previous researches. A general method is to deploy redundant resources, such as backup optical fibers and optical switches, such that the traffic load affected by a failure can be switched to the backup resources. Ref. [17] proposed to deploy backup devices and redundant feeder fibers to provide protection against failures in primary OLT and primary feeder fiber failures. Similarly, low-cost hybrid WDM/TDM passive optical networks (HPON) architecture is proposed to use extra infrastructure and equipment to support different levels of protection [18]. Deploying redundant components or fiber links is effective for enhancing protection, however, due to ultra-dense mm-wave RRHs deployment in 5G, it will require excessive cost to support mm-wave RRHs. Ring topologies with dual fiber paths have also been investigated to protect against ONU failures [19]. Survivable schemes for a DWDM ring networks are proposed in [20]. However, due to the ultra-dense RRH deployment, ring networks would require too much fibers and optical switches. Ref. [21] introduces a fiber access deployment strategy by overlapping multiple non-concentric areas to spread the load generated by a node failure over the network. The issue arises from this overlapping-coverage strategy for ultra-dense mm-wave RRHs is the serious border effects, in the sense that most external RRHs are not provided protection. Other research works [22], [23] focus on protecting the optical backhaul by alternative routes in the wireless frontend. For example, once a distribution fiber is broken, the traffic affected by this failure will be transferred into other available fibers using wireless multi-hop paths. Using the wireless multi-hop to transfer affected traffic in mm-wave accessing network in 5G C-RAN has also major shortcomings as: 1) traditional wireless routers do not have enough processing capacity for mm-wave signal transferring, and deploying mm-wave routers brings huge extra overhead; 2) mm-wave transmission is strongly directional and needs expensive pre-beamforming schemes for survivability management at each router. In 5G C-RAN, most existing researches on reliable network planning are focusing on the optimal BBU placement problem to protect against BBU failure [24], [25].

[1] It should be noted that in C-RAN the word *fronthaul* usually indicates the link between RRH and BBU, while the term *backhaul* refers to the backbone infrastructure connecting BBUs to the core network. However, this study only focuses on traffic assignment in mm-wave domain and does not adopt any function split/fronthaul interface in fiber links, so the type of fiber link (fronthaul or backhaul) does not have impact on our scheme. In our paper, we use the term *backhaul* to indicate the uplink fiber transmission originated from RRHs.

There have been also proposals for building green fiber-wireless access networks. Most of these works consider switching on/off network resources and using wireless routers for traffic transferring [26], [27]. Ref. [26] proposes to selectively shut down optical network unit (ONU) when in low-load state. Ref. [27] is focused on how to schedule a suitable sleep and wake-up times for ONUs. However, we cannot directly apply these schemes and approaches to mm-wave RRHs in 5G C-RAN for the same aforementioned reasons regarding wireless routers. At present, there are a few proposals on improving energy-efficiency in 5G C-RAN. Most of these focus on BBU-RRH dynamical resource mapping to save energy. The rationale is to switch off idle BBUs in BBU pool [28], [29]. Similarly, there are also some works putting RRHs with light load into sleep mode [30], [31]. In these works, if an RRH is switched-off, the power of neighboring RRHs is increased to extend the coverage, to establish connections with the mobile users and the traffic associated with the switched off RRH. However, when considering mm-wave RRHs in 5G C-RAN, it is difficult to extend the mm-wave coverage due to its high propagation loss characteristics.

To overcome the limitations disclosed above, our work focuses on utilizing free mm-wave links for real-time traffic assignment in RRHs that enables survivable and energy efficient backhaul transmission. There have been studies on cost-effective traffic assignment in small cells. In-band mm-wave technology that multiplex access traffic and interconnection in small cells is a promising option. Ref. [32] proposes a realistic deployment and traffic scheduling scheme for point-to-multipoint (PMP) in-band mm-wave data transmission. Ref. [33] develops a multipath-multihop (MPMH) scheme of in-band mm-wave transmission that achieves cost-effective and scalable deployment for varying picocell densities. Ref. [34] proposes to use free-space optical (FSO) communication for interconnecting small cells with lower overall latency and high data rate. Hybrid wireless/FSO technology has been also proposed to combine the advantages of both mm-wave and FSO [35], [36]. This paper differs from the aforementioned works, as in this paper, we propose a joint optimization framework to plan mm-wave RRHs placement that maximizing both backhaul survivability and energy efficiency.

B. CONTRIBUTIONS

The main novel technical contributions of this paper are summarized as follows:

1) We propose to use the same mm-wave frequency band both to provide end users access and to interconnect RRHs. In this scenario, leveraging traffic prediction obtained by a deep neural network, we propose a real-time traffic assignment scheme that is capable of i) rerouting traffic from an affected RRH to other RRHs to protect against backhaul failures, and ii) migrating traffic to as few RRHs as possible so that switching off some backhaul links for energy efficiency.
2) Due to the inherent short-range transmission of mm-wave, different RRH placement strategies can significantly affect the traffic assignment in RRHs. We present a joint optimization framework to optimally plan mm-wave RRHs placement, with the objective of maximizing both the number of survivable RRHs and switched-off backhaul links, based on integer linear programming (ILP).
3) To guarantee the scalability of the proposed scheme as network scale increases, we also present a heuristic algorithm, extended genetic algorithm (EGA), to provide a near-optimal solution.

The rest of the paper is organized as follows: Section II describes the network architecture and the mechanism of real-time traffic assignment scheme based survivable and energy efficient backhaul transmission. In Section III, we use ILP model to formulate the optimal mm-wave RRHs placement problem. The heuristic approach is proposed in Section IV. The simulation results are shown in Section V. Section VI concludes this paper.

II. TRAFFIC ASSIGNMENT SCHEME FOR SURVIVABLE AND ENERGY EFFICIENT BACKHAUL TRANSMISSION

In this Section, we first give a description of the considered 5G C-RAN network architecture with mm-wave RRHs. Then, we give an overview of the traffic prediction based real-time traffic assignment in RRHs for survivable and energy efficient backhaul transmission.

A. 5G C-RAN NETWORK ARCHITECTURE WITH MM-WAVE RRHS

While 5G is gradually developed and implemented, several heterogeneous wireless cellular architectures are presented, where macro cells use low frequency band to ensure large coverage and small cells exploit high frequency band to provide high-speed data access [37], [38]. Fig.1 shows the schematic of 5G C-RAN network with mm-wave RRHs considered in this paper, where mm-wave is used both to

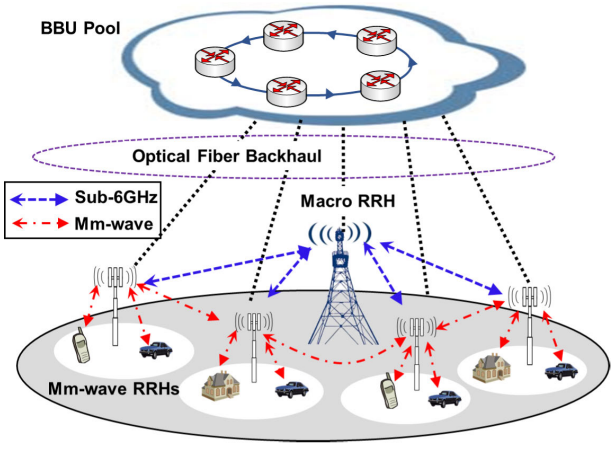

FIGURE 1. Schematic of 5G C-RAN network with mm-wave RRHs.

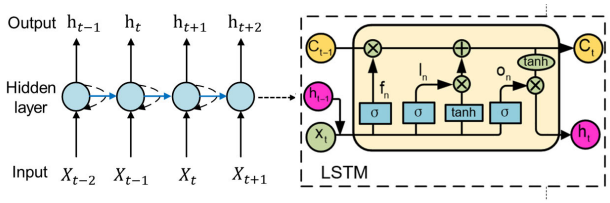

FIGURE 2. The detailed structure of a LSTM cell.

provide end users access and to interconnect RRHs for traffic assignment, which leads to energy saving thanks to hardware and frequency reuse. As shown in Fig. 1, we consider macro RRHs using frequency band below 6GHz to forward control signal (e.g., mm-wave beamforming precoding) from BBU pool both to end users and to other mm-wave RRHs. To support the enormous data transmission, we consider using fiber links for backhauling traffic. We assume each mm-wave RRH is assigned a unique optical wavelength as backhaul link, which is able to support the capacity of a mm-wave RRH.

B. TRAFFIC PREDICTION BASED SURVIVABLE AND ENERGY EFFICIENT BACKHAUL TRANSMISSION

In this section, we present a traffic prediction based survivable and energy-efficient backhaul transmission scheme, which uses free mm-wave links interconnecting RRHs. First, we give a description on the traffic prediction mechanism with LSTM network. Then we describe the real-time traffic assignment scheme about how to achieve survivable and energy efficient backhaul transmission.

1) TRAFFIC PREDICTION WITH LSTM NETWORK

As the input to our proposed real-time traffic assignment scheme, we use deep neural networks for traffic prediction. Recurrent neural network (RNN) is a deep learning algorithm that can be utilized to make predictions for the next time-series data. Long short-term memory (LSTM) network is an innovative RNN, which is proved to be an efficient tool for long-ranges dependencies modeling [39], [40]. LSTM works through storing message in the memory cell and forward it to the next time step. The detailed structure of a LSTM cell is described in Fig.2. The inputs to each LSTM cell include the new input x_t and the previous output h_{t-1}. Every time a new input x_t comes, it will be added to the memory cell by multiplying the value of input gate I_n. Similarly, the previous output h_{t-1} can be ''forgotten'' by multiplying the value of forget gate f_n. An output gate o_n is to transfer information from cell state C_t to the final state h_t.

Here, we assume long-term traffic of each RRH is collected and the cloud processor performs training of the LSTM network in the BBU pool. Then, giving traffic of multiple continuous time periods as inputs to LSTM, the traffic of each RRH at next time period can be predicted. The predicted traffic is then used to perform traffic assignment with our proposed approach, so achieving survivable and energy efficient backhaul transmission.

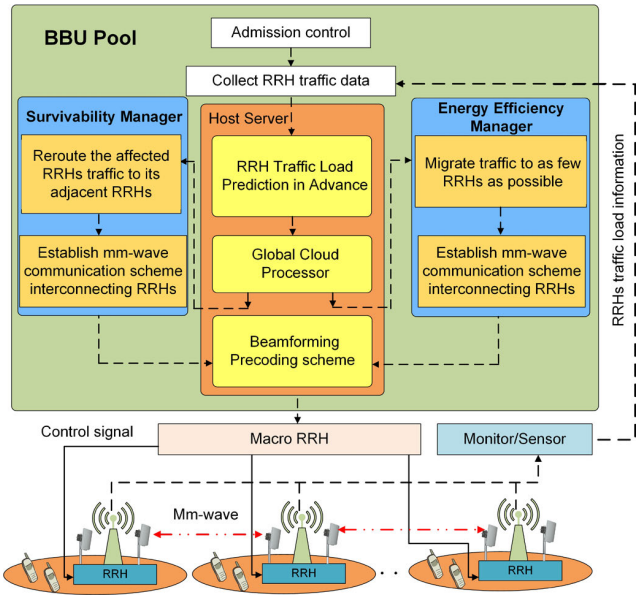

FIGURE 3. Proposed real time traffic assignment scheme.

2) TRAFFIC ASSIGNMENT MECHANISM FOR IMPROVING BACKHAUL SURVIVABILITY AND ENERGY EFFICIENCY

As shown in Fig. 3, the proposed traffic assignment scheme is supported by a cloud processor in BBU pool. Given the predicted traffic, the cloud processor will calculate a real-time traffic assignment for each RRH using free mm-wave links (i.e., links which are not connected to end users) to ensure backhaul survivability and improve energy efficiency. In particular, for backhaul survivability, the cloud processor plans the backup path for each RRH, such that each RRH knows in advance how to reroute the affected traffic to other RRHs if a fiber backhaul failure occurs. For energy efficiency, each RRH knows in advance how to migrate traffic to as few RRHs as possible at next time period to minimize the number of active backhaul links. Note that, the destination RRHs in the traffic assignment scheme should be within the maximum mm-wave transmission distance. Besides, in BBU pool, mm-wave beamforming precoding scheme on the traffic assignment are generated in advance, which are firstly sent to macro RRH, and then forwarded to mm-wave RRHs via control signal.

Due to tidal effects, each RRH has two options for backhauling its traffic at a specific time period: 1) using its own fiber backhaul link, and 2) switching off its own fiber backhaul link and using adjacent RRH's fiber backhaul link by migrating traffic towards it. In normal network condition (i.e., no failures), we keep fewest fiber backhaul links working to save energy. However, if failure occurs on a fiber of an RRH (currently receiving migrated traffic from other RRHs), traffic migration towards the affected RRH is immediately

suspended, and then this affected RRH can in turn reroute its traffic to other backup RRHs.

III. OPTIMAL PLACEMENT OF MM-WAVE RRHS FOR JOINTLY MAXIMIZING BACKHAUL SURVIVABILITY AND ENERGY EFFICIENCY

The above section provides a real-time traffic assignment scheme to improve backhaul survivability and energy efficiency. However, due to the inherent high propagation loss, mm-wave can be only used for short-range data transmission. Thus, RRH deployment significantly affects the possible interconnection of RRHs, which in turn affects the traffic assignment and leads to different backhaul survivability and energy efficiency. Therefore, it is extremely important to provide a proper RRHs placement. However, focusing only on the backhaul survivability and energy saving without considering network coverage and ignoring operator budget is impractical. Thus, our goal is to find the optimal placement of mm-wave RRHs to maximize backhaul survivability and energy efficiency, whilst meeting network coverage requirement and whilst considering a maximum budget in terms of number of RRH imposed by the operator. To evaluate backhaul survivability, we introduce the concept of survivable RRH, which indicates an RRH that can successfully reroute its affected traffic to backup RRHs after its associated backhaul-fiber failure at all time periods. The number of survivable RRHs is used as metric for backhaul survivability (the more survivable RRHs mean higher backhaul survivability). To evaluate energy efficiency, we compute the number of switched-off backhaul links (the more switched-off backhaul links, the higher energy efficiency can be achieved). We formalize the problem of mm-wave RRHs placement into an optimization model with the objective of jointly maximizing the number of survivable RRHs and the switched-off backhaul links, whilst meeting coverage requirement, based on ILP.

A. PROBLEM STATEMENT

The mm-wave RRHs placement problem in our work can be stated as follows: **Given** the network topology, coverage radius of mm-wave RRHs, the set of traffic pattern and maximum number of RRHs that can be supported per backhaul link, the coverage requirement ratio; **Decide** the optimal mm-wave RRHs placement scheme; **to maximize** the number of survivable RRHs and the number of switched-off backhaul links whilst meeting the coverage requirement, such that achieving maximum backhaul survivability and energy efficiency. We model this optimization problem using the following ILP.

B. ILP MODEL

1) INPUT SETS AND PARAMETERS

- I : set of locations for end users, and $|I|$ is the total number of end users.
- J : set of candidate locations for mm-wave RRHs, and $|J|$ is the number of candidate locations.
- N : number of mm-wave RRHs.
- C : capacity of mm-wave RRHs.
- R : coverage radius of mm-wave RRHs.
- T : set of time periods, including weekday time T_1 and weekend time T_2.
- $r_{t,j}$: traffic load in RRH j at time period t, where $j \in J$ and $t \in T$.
- $D_{i,j}$: distance between user i and RRH j, where $i \in I$ and $j \in J$.
- $T_{j,l}$: distance between RRH j and RRH l, where $j \in J$ and $l \in J$.
- Φ : maximum mm-wave transmission distance between RRHs.
- N_i : set of RRHs that covers user i, where $i \in I$ and $N_i = \{j \in J | D_{i,j} \leq R\}$.
- ω_j : set of RRHs that can interconnect with RRH j using mm-wave, where $j \in J$ and $\omega_j = \{l \in J | T_{j,l} \leq \phi\}$.
- h : maximum number of RRHs that can be supported per backhaul link.
- c : required network coverage ratio.

2) VARIABLES

The binary decision variables used in our proposed optimization framework are shown as follows.

- $u_i = \begin{cases} 1, & \text{if user } i \text{ is within the mm-wave coverage} \\ 0, & \text{otherwise} \end{cases}$
- $x_r = \begin{cases} 1, & \text{if RRH is placed at a candidate location } r \\ 0, & \text{otherwise} \end{cases}$
- $s_r = \begin{cases} 1, & \text{if RRH } r \text{ is a survivable RRH} \\ 0, & \text{otherwise} \end{cases}$
- $\gamma_{z,r} = \begin{cases} 1, & \text{if RRH } z \text{ is the backup RRH of RRH } r \\ 0, & \text{otherwise} \end{cases}$
- $\theta_{t,r} = \begin{cases} 1, & \text{if the backhaul link of RRH } r \text{ is working} \\ & \text{at time period } t \\ 0, & \text{otherwise} \end{cases}$
- $\delta_{t,l,j} = \begin{cases} 1, & \text{if the backhaul link of RRH } j \text{ is switched off and its traffic migrated to} \\ & \text{RRH } l \text{ at time period } t \\ 0, & \text{otherwise} \end{cases}$

3) OBJECTIVE FUNCTION

The objective function is given by:

$$\max F_T = \eta_1 \sum_{t \in T} \sum_{l \in J} \sum_{j \in J} \delta_{t,l,j} + \eta_2 \sum_{r \in J} s_r \quad (1)$$

The objective function has two parts: the component, $\sum_{t \in T} \sum_{l \in J} \sum_{j \in J} \delta_{t,l,j}$, captures the number of backhaul

links that can be switched off in all time periods in T, while $\sum_{r\in J} s_{t,r}$ represents the number of survivable RRHs. Here, we define an RRH as survivable only when its traffic can be successfully rerouted to its backup RRHs if failure occurs at all time periods in T. The two parts of objective function are linearly summed after multiplying them by the weighting factors η_1 and η_2 respectively, where the values of them can be adjusted to choose a primary objective. Besides, due to the difference between workday and weekend traffic model, the objective function can be further expressed as:

$$\max \alpha \cdot F_{T=T_1} + \beta \cdot F_{T=T_2} \tag{2}$$

where $F_{T=T_1}$ and $F_{T=T_2}$ are the objective values in workday T_1 and weekend T_2 respectively, which are summed by multiplying the weighting factors $\alpha = 5/7$ and $\beta = 2/7$ which are the ratio of workdays and weekends.

4) CONSTRAINTS

a) *RRH coverage constraints*: Equations (3) and (4) ensure that if an RRH is placed at a candidate location, it should cover at least one user. Equation (5) guarantees the placement of mm-wave RRHs should meet the coverage requirements.

$$u_i \le \sum\nolimits_{r\in N_i} x_r \quad \forall i \in I \tag{3}$$

$$u_i \ge \sum\nolimits_{r\in N_i} x_r / |I| \quad \forall i \in I \tag{4}$$

$$\sum\nolimits_{i\in I} u_i / |I| \ge c \tag{5}$$

b) *Network survivability constraints*: Equation (6) ensures that, if an RRH is identified as a survivable RRH, the sum of the remaining capacity of the backup RRHs should be greater than its own traffic load at any time period t. Noting that the backup RRHs should be within the maximum mm-wave transmission distance. Equation (7) imposes that if an RRH is not identified as a survivable RRH, its backup RRHs do not exist. Equation (8) and Equation (9) indicate that if an RRH is regarded as either a survivable RRH or backup RRH, it must be placed at a candidate location.

$$\sum\nolimits_{z\in\omega_r} \gamma_{z,r} \times (C - r_{t,r}) \ge s_r \times r_{t,r} \quad \forall t \in T\ \forall r \in J \tag{6}$$

$$\gamma_{z,r} \le s_r \quad \forall z \in J\ \forall r \in J \tag{7}$$

$$s_r \le x_r \quad \forall r \in J \tag{8}$$

$$\gamma_{z,r} \le x_z \quad \forall z \in J\ \forall r \in J \tag{9}$$

c) *Energy efficiency constraints*: Equation (10) guarantees that the sum of the traffic for an RRH and for other RRHs whose traffic is being migrated to it should be less than the capacity. It also should be noted that the distance between source and destination RRHs when traffic migration is applied should be within the maximum mm-wave transmission distance. Equation (11) ensures that the backhaul links should be in working state if there are traffic migrating to it. Equations (12), (13) and (14) indicate that both the source and destination RRHs should be placed at a candidate location, and the backhaul links should be either working or switched off.

$$\theta_{t,r} \times r_{t,r} + \sum\nolimits_{j\in\omega_j} \delta_{t,r,j} \times r_{t,j} \le C \forall t \in T\ \forall r \in J \tag{10}$$

$$\delta_{t,r,j} \le \theta_{t,r} \quad \forall t \in T\ \forall r \in J\ \forall j \in J \tag{11}$$

$$\theta_{t,r} \le x_r \quad \forall t \in\ \forall r \in J \tag{12}$$

$$\delta_{t,r,j} \le x_j \quad \forall t \in T\ \forall r \in J\ \forall j \in J \tag{13}$$

$$\sum\nolimits_{j\in J} \delta_{t,r,j} + r_{t,r} = x_r \quad \forall t \in T\ \forall r \in J \tag{14}$$

d) *Backhaul link capacity constraints*: Equations (15) limits the total number of RRH can be supported per backhaul link.

$$\sum\nolimits_{j\in J} \delta_{t,r,j} \le h \quad \forall t \in T,\ r \in J \tag{15}$$

e) *The number of RRHs constraints*: Equation (16) guarantee the number of mm-wave RRHs to be placed at candidate locations.

$$\sum\nolimits_{r\in J} x_r = N \tag{16}$$

IV. HEURISTIC ALGORITHM

As network scale increases, solving the ILP model becomes excessively time consuming. It is demonstrated that genetic algorithm (GA) is efficient to find multi-objective optimal solutions in one single simulation run [41], [42]. In this part, we propose a heuristic algorithm called *extended genetic algorithm* (EGA) for our proposed joint optimization scheme. Each individual is represented as a candidate solution for mm-wave RRHs placement. In the fitness function, we also propose an algorithm, namely *traffic assigned greedy energy-efficiency* (TAGE), to determine how to assign traffic in RRHs to maximize the number of switched-off backhaul links. Furthermore, we also give modified crossover operator and modified mutation operator. By iteratively implementing the genetic operators including selection, crossover, and mutation on the parent individuals to generate new individuals, the solutions for RRH placement can evolve toward better solutions.

For simplicity, we first introduce the notation used in EGA:

- P : initialized population
- N_p : population size
- L_n : the n-th individual, $n \in \{1, 2, .., N_p\}$
- G_k^n : the k-th gene in n-th individual, $k \in \{1, 2, \ldots, |J|\}$
- $E_{i,j}$: a binary value, taking 1 if user j is within the coverage of RRH i
- H_v^u : a binary value, taking 1 if mm-wave link connection is possible between RRHs u and v
- p_{cro} : crossover probability
- P_{mut} : mutation probability

1) *Individual and Population:* we represent each individual L_n as an RRH placement solution, in which G_k^n takes 1 if the RRH candidate location k hosts an RRH and 0 otherwise. Each individual is initialized by randomly selecting N genes taking value of '1' and others take value of '0'. The individual and population can be formulated as.

$$L_n = \left\{G_k^n \,|k= 1, \ldots, |J|\right\} \quad \forall n \in \left\{1, \ldots, N_p\right\} \tag{17}$$

$$P = \left\{L_n \,|n \in 1, \ldots, N_p\right\} \tag{18}$$

2) *Fitness Function*: we evaluate the fitness of available individuals according to a fitness function. The fitness function of EGA includes three parts: the number of survivable RRHs, the number of switched-off backhaul links, and a coverage penalty term. First, we study how to calculate the number of survivable RRHs as follows

$$Q_n^{t,v} = G_v^n \cdot \sum\nolimits_{u \in J} G_u^n \cdot H_v^u \cdot \left(C - r_{t,u}\right) \quad \forall t \in T, u, v \in J \tag{19}$$

$$sur_n^{t,v} = \begin{cases} 1, & \text{if } Q_n^{t,v} \geq r_{t,v} \\ 0, & \text{otherwise} \end{cases} \quad \forall t \in T, v \in J \tag{20}$$

Equations (19)-(20) determine if RRH v in L_n is capable of rerouting traffic to its backup RRHs at time period t. Specifically, Equation (19) calculates the total free capacity of the backup RRHs. Equation (20) determines whether backup RRHs have enough free capacity to totally receive traffic from RRH v at time period t.

$$sur_n^v = \left\lfloor \left(\sum\nolimits_{t \in T} sur_n^{t,v}\right)/\mathrm{T} \right\rfloor \quad \forall v \in J \tag{21}$$

Equation (21) determines if RRH v is a survivable RRH, which implies v can successfully reroute its traffic when backhaul failures occur in all time periods in T.

In the fitness function, maximizing the number of switched-off backhaul links is similar to a bin-packing problem (hence NP-hard), but with constraints like limited mm-wave transmission distance. Here, we propose an algorithm TAGE to determine how to assign traffic in RRHs to maximize the number of switched-off backhaul links. We introduce the concept of 'mm-wave connectivity' in TAGE, which can be defined as

$$Y_v^n = \sum\nolimits_{u \in J} H_u^v \quad \forall v \in J \tag{22}$$

where Y_v^n represents the number of RRHs that can establish mm-wave connections with RRH v. We define that the smaller Y_v^n, the lower 'mm-wave connectivity' of RRH v. The principle of our proposed TAGE algorithm is to preferentially determine the working state of the backhaul links, whose RRHs have lower mm-wave connectivity. In summary, we describe the detailed process of the TAGE algorithm as follows

We also introduce a coverage penalty term in the fitness function, which can be presented as follows:

$$cov\_penalty_n = \begin{cases} 1, & \text{if } \sum_{i \in I} cov_n^i / \,|I| < c \\ 0, & \text{otherwise} \end{cases} \tag{23}$$

Algorithm 1 TAGE Algorithm for Traffic Assignment in RRHs to Maximize Power Saving

Input: $r_{t,j} \forall t \in T, j \in J$; $Y_v^n \forall v \in J$;
RRH set: $U_n = \left\{G_v^n = 1 \,|v= 1, \ldots, |J|\right\} \forall L_n \in P$;
Output: RRH set $S_{t,n}$ whose backhaul link can be switched off at time period t; RRH set $W_{t,n}$ whose backhaul is working at time period t.

1. Sort U_n in ascending order according to the value of Y_v^n;
2. **while** $U_n \neq \emptyset$, **do**
3. $v \leftarrow$ pop-up top RRH in U_n.
4. **if** $v \in S_{t,n}$ or $v \in W_{t,n}$, **then**
5. Continue;
6. **else** find the RRH set:
   $\lambda_v^n = \left\{H_u^v = 1 \,|u \in \{1, \ldots, J\} \cap u \notin S_{t,n}\right\}$;
7. **if** $\lambda_v^n = \emptyset$
8. Add RRH v into $W_{t,n}$;
9. **else if** there exists RRHs set Q_x in λ_v^n whose traffic load satisfies: $\left\{r_{t,x} < r_{t,v} \cap r_{t,x} + r_{t,v} \leq C\right\}$;
10. Add v into $W_{t,n}$;
11. Sort Q_x in descending order according to the value of $r_{t,x}$;
12. **while** $Q_x \neq \emptyset$, **do**
13. $x \leftarrow$ pop-up top RRH in Q_x;
14. **if** $r_{t,x} > C - r_{t,v}$
15. Break;
16. **end if**
17. **if** $r_{t,x} \leq C - r_{t,v}$
18. Add x into $S_{t,n}$;
19. **end if**
20. Update $r_{t,v}$ by $r_{t,v} + r_{t,x}$;
21. **end while**
22. **else if** there exists RRHs set Z_x in λ_v^n whose traffic load satisfies: $\left\{r_{t,x} > r_{t,v} \cap r_{t,x} + r_{t,v} \leq C\right\}$
23. sort Z_x in descending order according to
24. the value of $r_{t,x}$
25. $x \leftarrow$ pop-up top RRH in Z_x.
26. Add x into $W_{t,n}$
27. Update $r_{t,v}$ by $r_{t,v} + r_{t,x}$;
28. **else if** all RRH x in λ_v^n whose traffic load satisfies: $\left\{r_{t,x} + r_{t,v} > C\right\}$
29. Add x into $W_{t,n}$
30. **end if**
31. **end if**
32. **end while**

where

$$\lambda_n^i = \sum\nolimits_{j \in J} E_{i,j} \quad \forall i \in I \tag{24}$$

$$cov_n^i = \begin{cases} 1, & \text{if } \lambda_n^i \geq 1 \\ 0, & \text{otherwise} \end{cases} \forall i \in I \tag{25}$$

Equation (24) calculates the number of RRHs that cover user i, while Equation (25) determines if user i is within the mm-wave coverage.

To sum up, we can formulate the fitness function as follows:

$$F(L_n) = \sigma \cdot \sum\nolimits_{v \in J} sur_n^v + \tau \cdot \sum\nolimits_{t \in T} S_{t,n} + \gamma \cdot cov\_penalty_n \tag{26}$$

where the three parts are linearly summed up by respectively multiplying the weighting factors σ, τ and γ, where the values of them can be adjusted to choose a primary objective.

3) *Genetic Operators*: The evolution is processed to create new populations by implementing genetic operators including selection, crossover, and mutation on the current population. The individuals of the next generation are selected from the current population by roulette wheel method. In particular, the probability of each individual entering to the next generation is equal to the proportion of its fitness value to the sum of fitness value for all individuals. Note that, in EGA, the fittest individual in the current generation does not implement selection operator and can go directly to the next generation.

Uniform crossover is not suitable in EGA due to the fact that individuals should guarantee the constraint in Equation (16) during the evolution, which implies that the number of genes with value of '1' should remain the same after crossover operators. Thus, we propose a modified crossover operator with the crossover probability p_{cro}. Specifically, to implement crossover operator for two individuals $L_m = \{G_1^m, \ldots, G_{N_p}^m\}$ and $L_n = \{G_1^n, \ldots, G_{N_p}^n\}$, we can randomly select crossover segments S_m and S_n from L_m and L_n as follows:

$$S_m = \left\{G_p^m, \ldots, G_q^m\right\} \quad \forall p,\ q \in \left\{1, \ldots .N_p\right\},\ p < q \tag{27}$$

$$S_n = \left\{G_p^n, \ldots, G_q^n\right\} \quad \forall p,\ q \in \left\{1, \ldots .N_p\right\},\ p < q \tag{28}$$

The procedure for our proposed modified crossover operator is described in Algorithm 2.

To increase population diversity, we also implement a modified mutation operator with the mutation probability p_{mut}. For an individual $L_m = \{G_1^m, \ldots, G_{N_p}^m\}$, we implement the mutation by randomly selecting genes to change their values. Note that the mutation operator also needs to guarantee the constraint in Equation (16), if the mutation operator changes a gene '0' to be '1', another gene '1' in L_m needs to be randomly selected and changed to be '0'; In a similar way, if a gene '1' is changed to be '0', another gene '0' in L_m needs to be changed to be'1'. With the genetic operators above, we continuously create new populations. Finally, we can obtain the fittest individual representing the optimal mm-wave RRHs placement scheme from the last population.

In terms of time complexity, EGA requires the computation of the number of survivable RRHs and switched-off backhaul links that have complexity of O($|J|$) for each individual, and $O\ (N_p \cdot |J|)$ for all individual, where $|J|$ is the number of candidate locations and N_p is the population size. Time complexity of the penalty term is $O\ (N_p)$. Since the cost of crossover and mutation is a fixed value, such values are not considered in accounting for time complexity. Therefore, the total time complexity of EGA is of the order $O\ (N_p \cdot |J|)$.

Algorithm 2 Modified Crossover Operator

Input: L_m, L_n, S_m, S_n, $\varepsilon_m = \sum_{m \in \{1,\ldots,q-p\}} S_m$
$\varepsilon_n = \sum_{n \in \{1,\ldots,q-p\}} S_n$, $\forall m, n \in J$
Output: Individuals after crossover: L_m^{new}, L_n^{new}
1. Randomly generate o_c= rand(0, 1)
2. **while** $o_c \leq p_{cro}$
3. exchange S_m, S_n to generate new individuals L_m^{new} and L_n^{new}.
4. **if** $\varepsilon_n > \varepsilon_m$
5. Update $\left\{L_m^{new} - S_m\right\}$ in L_m^{new} by randomly selecting $\varepsilon_n - \varepsilon_m$ genes '0' to be '1';
6. Update $\left\{\mathrm{L_n^{new}} - \mathrm{S_n}\right\}$ in L_n^{new} by randomly selecting $\varepsilon_n - \varepsilon_m$ genes '1' to be '0';
7. **else if**$\varepsilon_n < \varepsilon_m$
8. Update $\left\{L_m^{new} - S_m\right\}$ in L_m^{new} by randomly selecting $\varepsilon_n - \varepsilon_m$ genes '1' to be '0';
9. Update $\left\{L_n^{new} - S_n\right\}$ in L_n^{new} by randomly selecting $\varepsilon_n - \varepsilon_m$ genes '0' to be '1';
10. **else if** $\varepsilon_n = \varepsilon_m$
11. output L_m^{new}, L_n^{new}
12. **end if**
13. **end while**

V. ILLUSTRATIVE NUMERICAL EXAMPLES

A. SIMULATION ENVIRONMENT

In our simulations, we test the proposed optimization scheme in a dense urban area covering 1.2 × 1.2 square kilometers. We show an example in Fig. 4, where the whole area is divided into 36 0.2 × 0.2 km grids. One candidate location for mm-wave RRH is randomly distributed in each grid as a red plus. A macro RRH is placed at the center of the simulation area as a red triangle. To emulate a real deployment, 300 users are randomly distributed as blue dots. We assume there is no obstruction between RRH and end users, such that each RRH can establish mm-wave link with the end users within mm-wave coverage. The number of mm-wave RRH is usually determined by operator's budget, here, we assume the number of mm-wave RRHs to be placed in the area is 23. We suppose all antennas in mm-wave RRHs are omnidirectional, i.e., they can generate beams with different directions, and a coverage radius of 200m[2]. As RRHs are generally deployed at high locations, i.e. roofs and light poles, we assume few obstructions between RRHs, and set the maximum mm-wave transmission distance for interconnecting RRHs to be 300m. The optimization is implemented on a PC of Inter(R) Xeon(R)

[2]Ref. [11] has confirmed that for mm-wave cellular sizes on the order of 200m, atmospheric absorption and rain attenuation in urban environment does not create significant path loss for mm-wave, particularly at 28GHz and 38GHz. Ref. [12] also indicates that for small distance (less than 1km), rain attenuation presents a minimal effect on the propagation of mm-wave.

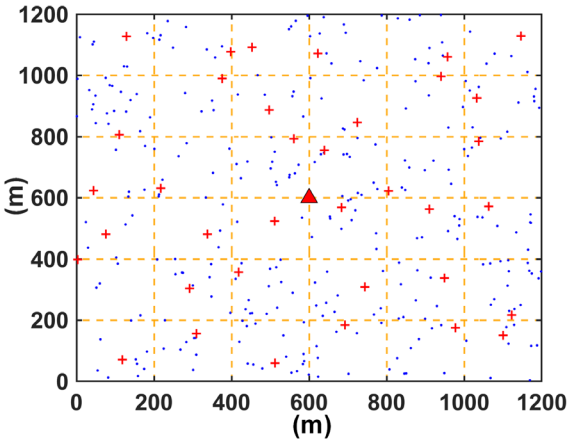

FIGURE 4. Deployment scenario with mm-wave RRHs candidate locations randomly distributed.

CPU E5-2630 V4 @2.20GHz & 2.20GHz and 128GB RAM and solved in Matlab/Yalmip environment, using Gurobi solver.

B. TRAFFIC LOAD PREDICTION

The traffic data analyzed in this paper comes from an European Telecom operator, Telecom Italia, as part of the ''Big Data Challenge'' [43]. The data set refers to the time series of aggregated cell phone traffic, including short message services (SMS), call service and Internet traffic activity, sent and received by end users for each squared cell of the Milan area, measured during November 2013. As mm-wave traffic is discussed in this paper, we randomly select 36 traffic patterns from the data set and linearly scale them close to the throughput of mm-wave RRHs, which are assumed to represent the total traffic collected within mm-wave RRHs coverage [1], [44].

In this part, we evaluate the performance of LSTM based traffic prediction. The time t of the LSTM network is in interval of 30 minutes. Using the LSTM network, the traffic can be predicted 30 minutes in advance. In particular, an LSTM network is trained with 1104 data samples for 23 days and tested by 336 data samples for 7 days. Stochastic gradient descent is used for training, while the training data is broken into batches of 30 samples and go through 2000 epochs. Truncated back propagation through time (TBPTT) is utilized for optimizing the weight parameters. In the simulation, 8 time steps $X_t = \{x_{t-7}, x_{t-6}, \ldots, x_t\}$ are used. We give an example in Fig.5 of the traffic prediction performance which implies (a) office dominant area, (b) residential dominant area, and (c) entertainment dominant area respectively. As shown in Fig. 5, the test data set obtains a mean absolute error (MAE) of 0.59 Gbps, mean absolute percentage error (MAPE) of 6.1%, and a root means square error (RMSE) of 0.71Gbps, which indicate the LSTM network is trustworthy to make accurate traffic predictions.

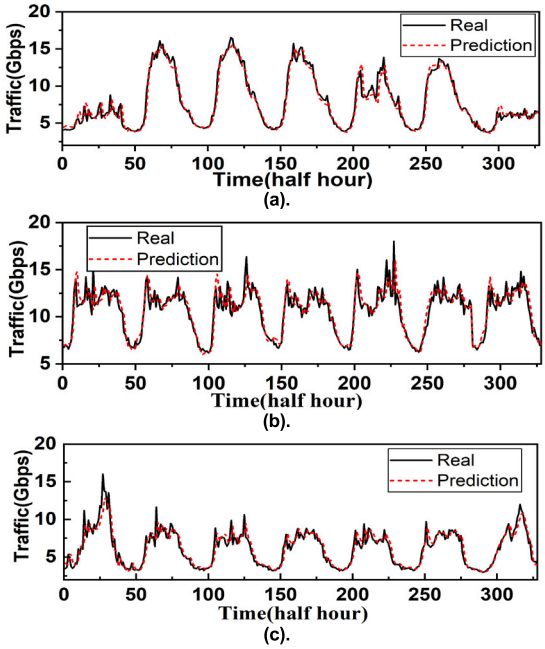

FIGURE 5. LSTM based traffic prediction performance. (a) Office dominant area. (b) Residential dominant area. (c) Entertainment dominant area.

C. EVALUATION METRICS FOR THE OPTIMAL RRH PLACEMENT

To plan the optimal mm-wave RRH placement, we consider two days of traffic profiles per RRH (a weekday and a weekend day) to represent the typical long-term traffic profiles. The peak traffic in the considered traffic profiles is 20Gbps. To evaluate the performance of both the ILP and EGA, we quantify the backhaul survivability in terms of percentage of survivable RRHs (defined in Equation. (6)) P_s. For backhaul energy efficiency, we calculate the percentage of switched-off backhaul links (defined in Equation. (10)) P_e (the more switched-off backhaul links, the higher energy efficiency.

D. NUMERICAL RESULTS

In this subsection, we will show the results for the optimal mm-wave RRHs placement, and evaluate the performance of backhaul survivability ratio P_s and energy efficiency ratio P_e respectively.

1) OPTIMAL MM-WAVE RRHS PLACEMENT SOLUTIONS

Our optimization scheme (a) identifies the optimal deployment locations of mm-wave RRHs from the set of candidate locations, with the objective of maximizing the value of both P_s and P_e; (b) identifies the associated traffic assignment in RRHs. As an example, we assume RRH capacity C = 22Gbps and maximum mm-wave transmission distance $\emptyset$ = 300m to interconnect RRHs, Fig. 6 (a) and (b) show the optimal mm-wave RRHs placement solutions for required coverage ratio R_c of 100% and 98% respectively. In Fig. 6, we denote survivable RRHs by red circles (i.e., an RRH can

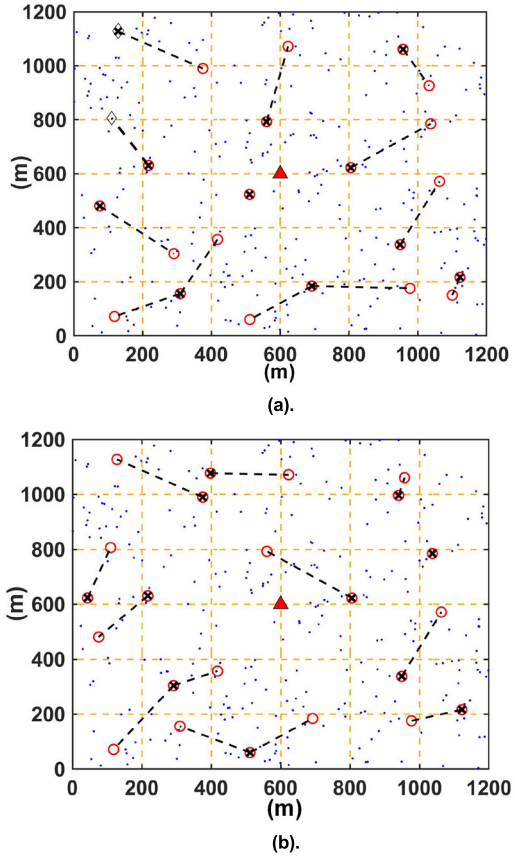

FIGURE 6. Optimal RRH placement solutions with (a) coverage ratio requirement 100%, (b) coverage requirement 98%.

successfully reroute its affected traffic to backup RRHs after its associated backhaul-fiber failure at all time periods), and others by black diamonds. For simplicity, we do not present the backup path for each RRH in Fig. 6. Besides, we use black crosses to denote an RRH whose backhaul link is active at 10a.m on the weekday, and the black dot lines denote the real-time traffic migration path from an RRH whose backhaul link is switched-off to an RRH whose backhaul link is active. As shown in Fig. 6, the isolated black crosses indicate that some RRHs' backhaul links are active, but with no traffic from other RRHs migrating towards it, which is due to they do not have enough free mm-wave capacity to support other RRHs. The maximum P_s achieved by the RRH placement shown in Fig. 6(a) is 91.3%, while the maximum P_e is 51.8%. In Fig. 6(b), the maximum P_s is 100%, while the maximum P_e is 56.1%.

2) ANALYSIS OF SURVIVABILITY

In this subsection, we apply the ILP and EGA to evaluate the backhaul survivability of the optimal mm-wave RRHs placement. We consider three mm-wave transmission distances ($\phi = 200$m,$\phi = 250$m, and $\phi = 300$m) to interconnect RRHs. Assuming 100% coverage ratio required, Fig. 7 presents the backhaul survivability ratio P_s for different

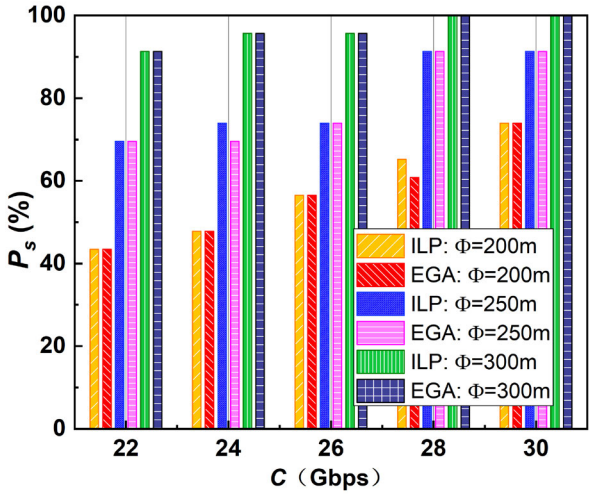

FIGURE 7. Survivability ratio for increasing RRH capacity.

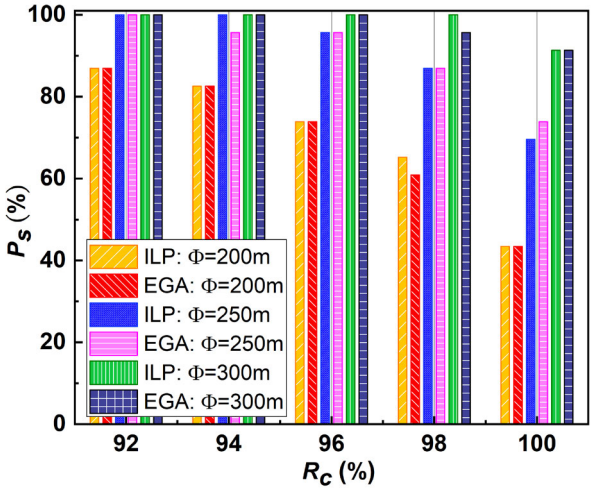

FIGURE 8. Survivability ratio for different required coverage ratio.

RRH capacity C. As expected, P_s increases as C increases. The reason is that a larger C brings more free mm-wave resources to reroute traffic to protect against backhaul failures. When C increases from 22Gbps to 30Gbps, the survivability ratio increases 30.5%, 21.8%, and 8.7% for $\phi = 200$m,$\phi = 250$m, and $\phi = 300$m respectively. We can also observe that EGA provides very close results.

Fig. 8 provides the ILP and EGA results on backhaul survivability ratio P_s for different coverage ratio R_c. Assuming the RRH capacity $C = 22$ Gbps, we can see that the increasing R_c leads to the decrease of P_s. When R_c increases from 92% to 100%, the value of P_s decreases 43.5%, 30.5%, and 8.7% for $\phi = 200$m,$\phi = 250$m, and $\phi = 300$m, respectively, which indicates that a larger ϕ reduces the impact of the increasing coverage requirement on backhaul survivability performance. Also in this case, the EGA results are very close to the ILP.

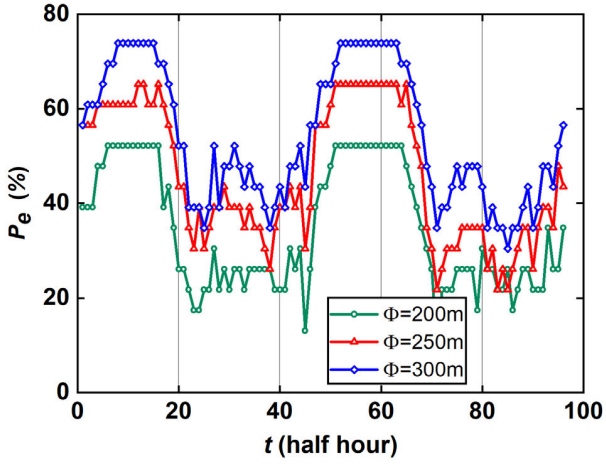

FIGURE 9. Ratio of backhaul links to be switched off in two days for ϕ= 200, 250 300m.

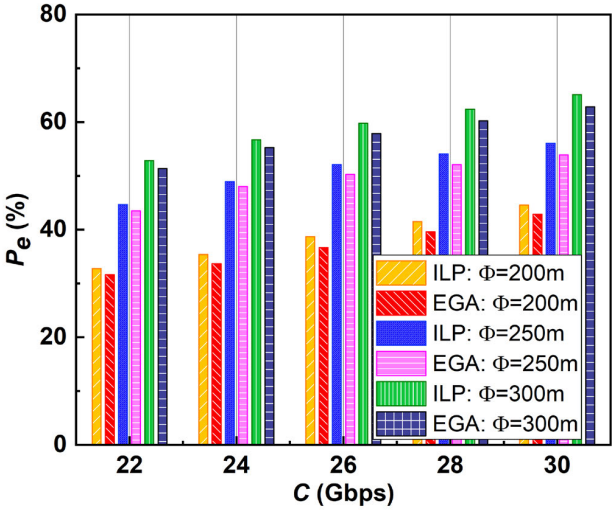

FIGURE 10. Ratio of switched backhaul links for increasing RRH capacity.

3) ANALYSIS OF ENERGY EFFICIENCY

In this subsection, we use both ILP and EGA to evaluate the backhaul energy efficiency. Assuming RRH capacity C = 22Gbps and coverage requirement R_c = 100%, we show the value of P_e (ratio of switched-off backhaul links) every half-hour period during two days in Fig. 9 (only ILP results are presented for simplicity). In Fig. 9, time periods from 1 to 48 represent a weekday and time periods from 49 to 98 represent weekend day. It is evident that a larger ϕ leads to higher P_e, as RRHs can establish more mm-wave interconnections with adjacent RRHs. We can also observe from Fig. 9 that P_e in daytime is lower that at night, since, as tidal effects, most RRHs have little free capacity in daytime. Furthermore, average value of P_e is about 2% higher on weekend day than on workday.

Fig. 10 presents the backhaul energy efficiency ratio P_e obtained by ILP and EGA for increasing RRH capacity C when the coverage requirement ratio R_c = 100%. It can be observed that the value of P_e increases as C increases. When C increase from 22Gbps to 30Gbps, the value of P_e increases 11.8%, 11.4%, and 12.3% for ϕ = 200m, ϕ = 250m and ϕ = 300m respectively, which is similar to the survivability trends, as larger capacity brings more free mm-wave resources to implement traffic migration in RRHs. As shown in Fig. 10, EGA also provides close results, with the value of P_e 3.5% lower than ILP.

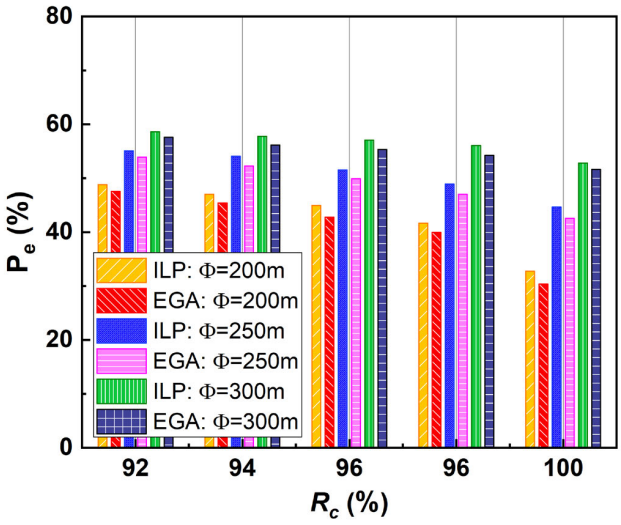

FIGURE 11. Ratio of switched backhaul links for increasing coverage ratio requirements.

Fig 11 shows the backhaul energy efficiency ratio P_e for increasing coverage requirement R_c. For increasing R_c, the value of P_e decreases for different mm-wave transmission distances ϕ = 200m, ϕ = 250m and ϕ = 300m, which indicates a trade-off between energy efficiency and coverage requirement. When R_c increases from 92% to 100%, the value of P_e decrease 16.1%, 10.4%, and 5.8% for ϕ = 200m, ϕ = 250m and ϕ = 300m respectively. Fig. 11 also shows that EGA provides close results, with P_e 3.3% lower than ILP.

As operators may have specific backhaul survivability requirements, we might need to prioritize survivability improvement for the optimal mm-wave RRHs placement. Here, we evaluate the impact of increasing survivability requirements on backhaul energy efficiency. In both ILP and EGA, by adjusting weight factors of the two optimization objectives, we can obtain backhaul energy efficiency ratio P_e while ensuring specific survivability ratio P_s. Assuming RRH capacity C = 22Gbps, Fig. 12 shows that, for P_s increasing from 70% to 100%, the value of P_e decreases 1.9%, 0.17% and 0.15% for ϕ = 200m, ϕ = 250m, and ϕ = 300m respectively, which indicates that larger ϕ leads to slight impact of the increasing survivability requirements on backhaul energy efficiency. This is because larger ϕ can provide more mm-wave links to interconnect RRHs, such that high survivability requirements can be easily achieved and impact slightly on RRH placement solutions, which in turn decrease the impact on backhaul energy efficiency.

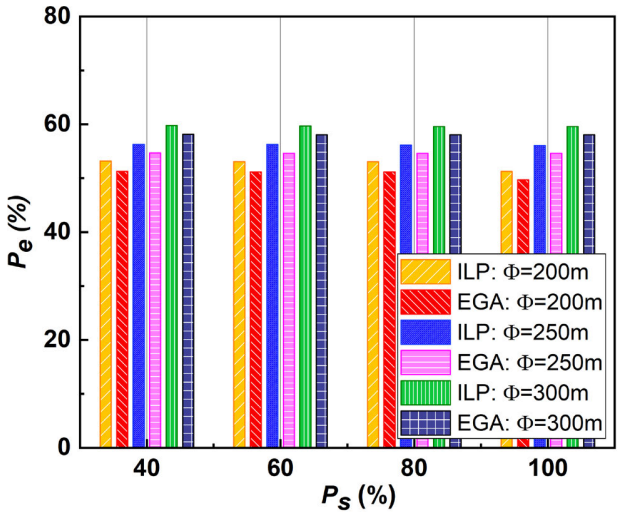

FIGURE 12. Ratio of switched backhaul links for increasing survivability ratio.

VI. CONCLUSION

Establishing a reliable and energy efficient backhaul connectivity for ultra-dense mm-wave RRHs is an important in 5G. In this study, we show how to optimally place mm-wave RRHs to jointly maximize survivability and energy efficiency. We propose to use free mm-wave resources for traffic assignment in RRHs, which leads to energy saving and increase survivability thanks to hardware and frequency reuse. We developed an ILP model and a genetic algorithm called EGA which act as a guideline for optimal mm-wave RRHs placement. We simulate both the ILP and EGA under a dense urban area. In our illustrative numerical results, we give examples of optimal mm-wave RRH placement and discuss the effects of RRH capacity, coverage requirement, and maximum mm-wave transmission distance on the optimization. We also observe that EGA results are very close to those of the ILP, which demonstrate the effectiveness of the proposed heuristic approach for larger-scale network.

As future work on this topic, we plan to incorporate multi-hop interconnections in mm-wave RRHs while considering latency constraints.

REFERENCES

[1] M. Shafi, A. F. Molisch, P. J. Smith, T. Haustein, P. Zhu, P. De Silva, F. Tufvesson, A. Benjebbour, and G. Wunder, "5G: A tutorial overview of standards, trials, challenges, deployment, and practice," *IEEE J. Sel. Areas Commun.*, vol. 35, no. 6, pp. 1201–1221, Jun. 2017.

[2] F. Boccardi, R. W. Heath, A. Lozano, T. L. Marzetta, and P. Popovski, "Five disruptive technology directions for 5G," *IEEE Commun. Mag.*, vol. 52, no. 2, pp. 74–80, Feb. 2014.

[3] "C-RAN: The road towards green RAN, v.2.5," China Mobile Res. Inst., Beijing, China, White Paper, Oct. 2011.

[4] A. Checko, H. L. Christiansen, Y. Yan, L. Scolari, G. Kardaras, M. S. Berger, and L. Dittmann, "Cloud RAN for mobile networks—A technology overview," *IEEE Commun. Surveys Tuts.*, vol. 17, no. 1, pp. 405–426, 1st Quart., 2015.

[5] F. Musumeci, C. Rottondi, A. Nag, I. Macaluso, D. Zibar, M. Ruffini, and M. Tornatore, "An overview on application of machine learning techniques in optical networks," *IEEE Commun. Surveys Tuts.*, vol. 21, no. 2, pp. 1383–1408, 2nd Quart., 2019.

[6] A. Yu, H. Yang, W. Bai, L. He, H. Xiao, and J. Zhang, "Leveraging deep learning to achieve efficient resource allocation with traffic evaluation in datacenter optical networks," in *Proc. Opt. Fiber Commun. Conf. Expo. (OFC)*, Mar. 2018, pp. 1–3.

[7] W. Mo, C. L. Gutterman, Y. Li, G. Zussman, and D. C. Kilper, "Deep neural network based dynamic resource reallocation of BBU pools in 5G C-RAN ROADM networks," in *Proc. Opt. Fiber Commun. Conf. Expo. (OFC)*, Mar. 2018, pp. 1–3.

[8] N. Fernández, R. J. D. Barroso, D. Siracusa, A. Francescon, I. de Miguel, E. Salvadori, J. C. Aguado, and R. M. Lorenzo, "Virtual topology reconfiguration in optical networks by means of cognition: Evaluation and experimental validation [invited]," *IEEE/OSA J. Opt. Commun. Netw.*, vol. 7, no. 1, pp. A162–A173, Jan. 2015.

[9] J. Karjalainen, M. Nekovee, H. Benn, W. Kim, J. Park, and H. Sungsoo, "Challenges and opportunities of mm-wave communication in 5G networks," in *Proc. 9th Int. Conf. Cognit. Radio Oriented Wireless Netw.*, Jun. 2014, pp. 372–376.

[10] S. Akoum, O. El Ayach, and R. W. Heath, "Coverage and capacity in mmWave cellular systems," in *Proc. Conf. Rec. Forty 6th Asilomar Conf. Signals, Syst. Comput. (ASILOMAR)*, Nov. 2012, pp. 688–692.

[11] T. S. Rappaport, S. Sun, R. Mayzus, H. Zhao, Y. Azar, K. Wang, G. N. Wong, J. K. Schulz, M. Samimi, and F. Gutierrez, "Millimeter wave mobile communications for 5G cellular: It will work!," *IEEE Access*, vol. 1, pp. 335–349, 2013.

[12] W. Roh, J.-Y. Seol, J. Park, B. Lee, J. Lee, Y. Kim, J. Cho, K. Cheun, and F. Aryanfar, "Millimeter-wave beamforming as an enabling technology for 5G cellular communications: Theoretical feasibility and prototype results," *IEEE Commun. Mag.*, vol. 52, no. 2, pp. 106–113, Feb. 2014.

[13] X. Xia, K. Xu, Y. Wang, and Y. Xu, "A 5G-enabling technology: Benefits, feasibility, and limitations of in-band full-duplex mMIMO," *IEEE Veh. Technol. Mag.*, vol. 13, no. 3, pp. 81–90, Sep. 2018.

[14] C.-Y. Chang, N. Nikaein, R. Knopp, T. Spyropoulos, and S. S. Kumar, "FlexCRAN: A flexible functional split framework over Ethernet fronthaul in cloud-RAN," in *Proc. IEEE Int. Conf. Commun. (ICC)*, May 2017, pp. 1–7.

[15] C.-L. I, J. Huang, R. Duan, C. Cui, J. Jiang, and L. Li, "Recent progress on C-RAN centralization and cloudification," *IEEE Access*, vol. 2, pp. 1030–1039, 2014.

[16] F. Musumeci, C. Bellanzon, N. Carapellese, M. Tornatore, A. Pattavina, and S. Gosselin, "Optimal BBU placement for 5G C-RAN deployment over WDM aggregation networks," *J. Lightw. Technol.*, vol. 34, no. 8, pp. 1963–1970, Apr. 15, 2016.

[17] B. Kantarci and H. T. Mouftah, "Availability and cost-constrained long-reach passive optical network planning," *IEEE Trans. Rel.*, vol. 61, no. 1, pp. 113–124, Mar. 2012.

[18] M. Mahloo, J. Chen, L. Wosinska, A. Dixit, B. Lannoo, D. Colle, and C. M. Machuca, "Toward reliable hybrid WDM/TDM passive optical networks," *IEEE Commun. Mag.*, vol. 52, no. 2, pp. S14–S23, Feb. 2014.

[19] M. M. Carvalho and E. A. De Souza, "A novel protection mechanism in TDM-PON," in *Proc. 11th Int. Conf. Transparent Opt. Netw.*, Jun. 2009, pp. 1–4.

[20] E. Wong, E. Grigoreva, L. Wosinska, and C. M. Machuca, "Enhancing the survivability and power savings of 5G transport networks based on DWDM rings," *J. Opt. Commun. Netw.*, vol. 9, no. 9, pp. D74–D85, Sep. 2017.

[21] M. Ruffini, D. Mehta, B. O'Sullivan, L. Quesada, L. Doyle, and D. Payne, "Deployment strategies for protected long-reach PON," *IEEE/OSA J. Opt. Commun. Netw.*, vol. 4, no. 2, pp. 118–129, Feb. 2012.

[22] N. Ghazisaidi, M. Scheutzow, and M. Maier, "Survivability analysis of next-generation passive optical networks and fiber-wireless access networks," *IEEE Trans. Rel.*, vol. 60, no. 2, pp. 479–492, Jun. 2011.

[23] N. Correia, J. Coimbra, and G. Schütz, "Fault-tolerance planning in multiradio hybrid wireless optical broadband access networks," *IEEE/OSA J. Opt. Commun. Netw.*, vol. 1, no. 7, pp. 645–654, Dec. 2009.

[24] B. M. Khorsandi, C. Raffaelli, M. Fiorani, L. Wosinska, and P. Monti, "Survivable BBU hotel placement in a C-RAN with an optical WDM transport," in *Proc. DRCN Design Reliable Commun. Netw.*, Munich, Germany, Mar. 2017, pp. 1–6.

[25] M. Shehata, F. Musumeci, and M. Tornatore, "Resilient BBU placement in 5G C-RAN over optical aggregation networks," *Photonic Netw. Commun.*, vol. 37, no. 3, pp. 388–398, Jan. 2019.

[26] P. Chowdhury, M. Tornatore, S. Sarkar, and B. Mukherjee, "Building a green wireless-optical broadband access network (WOBAN)," *J. Lightw. Technol.*, vol. 28, no. 16, pp. 2219–2229, Aug. 2010.

[27] Y. Yan, S.-W. Wong, L. Valcarenghi, S.-H. Yen, D. R. Campelo, S. Yamashita, L. Kazovsky, and L. Dittmann, "Energy management mechanism for Ethernet passive optical networks (EPONs)," in *Proc. IEEE Int. Conf. Commun.*, May 2010, pp. 1–5.

[28] Y. Li, M. Bhopalwala, S. Das, J. Yu, W. Mo, M. Ruffini, and D. C. Kilper, "Joint optimization of BBU pool allocation and selection for C-RAN networks," in *Proc. Opt. Fiber Commun. Conf. Expo. (OFC)*, Mar. 2018, pp. 1–3.

[29] R. I. Tinini, D. M. Batista, G. B. Figueiredo, M. Tornatore, and B. Mukherjee, "Low-latency and energy-efficient BBU placement and VPON formation in virtualized cloud-fog RAN," *J. Opt. Commun. Netw.*, vol. 11, no. 4, p. B37, Apr. 2019.

[30] C. Pan, H. Zhu, N. J. Gomes, and J. Wang, "Joint precoding and RRH selection for user-centric green MIMO C-RAN," *IEEE Trans. Wireless Commun.*, vol. 16, no. 5, pp. 2891–2906, May 2017.

[31] N. Saxena, A. Roy, and H. Kim, "Traffic-aware cloud RAN: A key for green 5G networks," *IEEE J. Sel. Areas Commun.*, vol. 34, no. 4, pp. 1010–1021, Apr. 2016.

[32] R. Taori and A. Sridharan, "Point-to-multipoint in-band mmwave backhaul for 5G networks," *IEEE Commun. Mag.*, vol. 53, no. 1, pp. 195–201, Jan. 2015.

[33] S. Saadat, D. Chen, and T. Jiang, "Multipath multihop mmWave backhaul in ultra-dense small-cell network," *Digit. Commun. Netw.*, vol. 4, no. 2, pp. 111–117, Apr. 2018.

[34] M. Alzenad, M. Z. Shakir, H. Yanikomeroglu, and M.-S. Alouini, "FSO-based vertical Backhaul/Fronthaul framework for 5G+ wireless networks," *IEEE Commun. Mag.*, vol. 56, no. 1, pp. 218–224, Jan. 2018.

[35] H. Dahrouj, A. Douik, F. Rayal, T. Y. Al-Naffouri, and M.-S. Alouini, "Cost-effective hybrid RF/FSO backhaul solution for next generation wireless systems," *IEEE Wireless Commun.*, vol. 22, no. 5, pp. 98–104, Oct. 2015.

[36] A. Douik, H. Dahrouj, T. Y. Al-Naffouri, and M.-S. Alouini, "Hybrid radio/free-space optical design for next generation backhaul systems," *IEEE Trans. Commun.*, vol. 64, no. 6, pp. 2563–2577, Jun. 2016.

[37] X. Ge, H. Cheng, M. Guizani, and T. Han, "5G wireless backhaul networks: Challenges and research advance," *IEEE Netw.*, vol. 28, no. 6, pp. 6–11, Nov. 2014.

[38] K. Sakaguchi, G. K. Tran, H. Shimodaira, S. Nanba, T. Sakurai, K. Takinami, E. C. Strinati, A. Capone, I. Karls, R. Arefi, and T. Haustein, "Millimeter-wave evolution for 5G cellular networks," *IEICE Trans. Commun.*, vol. 98, no. 3, pp. 388–402, Mar. 2015.

[39] F. A. Gers, J. Schmidhuber, and F. Cummins, "Learning to forget: Continual prediction with LSTM," *Neural Comput.*, vol. 12, no. 10, pp. 2451–2471, Oct. 2000.

[40] S. Xingjian, Z. Chen, H. Wang, D.-Y. Yeung, W.-K. Wong, and W.-C. Woo, "Convolutional LSTM network: A machine learning approach for precipitation nowcasting," in *Proc. NIPS*, Jun. 2015, pp. 802–810.

[41] I. de Miguel, R. Vallejos, A. Beghelli, and R. J. Durán, "Genetic algorithm for joint routing and dimensioning of dynamic WDM networks," *IEEE/OSA J. Opt. Commun. Netw.*, vol. 1, no. 7, pp. 608–621, Dec. 2009.

[42] R. Morais, C. Pavan, A. Pinto, and C. Requejo, "Genetic algorithm for the topological design of survivable optical transport networks," *IEEE/OSA J. Opt. Commun. Netw.*, vol. 3, no. 1, pp. 17–26, Jan. 2011.

[43] S. Troia, G. Sheng, R. Alvizu, G. A. Maier, and A. Pattavina, "Identification of tidal-traffic patterns in metro-area mobile networks via matrix factorization based model," in *Proc. IEEE Int. Conf. Pervas. Comput. Commun. Workshops (PerCom Workshops)*, Mar. 2017, pp. 297–301.

[44] "NGMN 5G white paper, v.1.0," Next Gener. Mobile Netw. Alliance, Frankfurt, Germany, Feb. 2015.

BO TIAN received the B.S. degree in electronic engineering from Xidian University, Xian, China, in 2015. He is currently pursuing the Ph.D. degree in electronic science and technology from the Beijing University of Posts and Telecommunications (BUPT), Beijing, China. His research interests include 5G RAN transport networks, converged optical, and wireless networks.

QI ZHANG received the Ph.D. degree from the Beijing University of Posts and Telecommunications (BUPT), Beijing, China, in 2005. She is currently a Professor with the School of Electric Engineering, BUPT. Her research interests include optical access networks, optical fiber communication, and satellite communication. Within this area, she has authored or coauthored more than 60 SCI and EI articles.

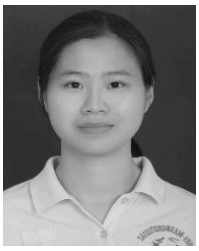

YIQIANG LI received the B.S. degree in electronic engineering from Xiangtan University, Xiangtan, China, in 2016. She is currently pursuing the Ph.D. degree in electronic science and technology from the Beijing University of Posts and Telecommunications (BUPT), Beijing, China. Her research interests include elastic optical networks and software-defined optical networks.

MASSIMO TORNATORE (Senior Member, IEEE) received the Ph.D. degree from Politecnico di Milano, in 2006. He is currently an Associate Professor with the Department of Electronics, Information, and Bioengineering, Politecnico di Milano. He also holds an appointment as an Adjunct Professor with the University of California at Davis, Davis, CA, USA, and as a Visiting Professor with the University of Waterloo, Waterloo, ON, Canada. His research interests include performance evaluation, optimization, and design of communication networks (with an emphasis on the application of optical networking technologies), cloud computing, and machine learning application for network management. He is a member of the Editorial Board of the IEEE COMMUNICATIONS SURVEYS AND TUTORIALS, the IEEE COMMUNICATIONS LETTERS, *Photonic Network Communications* (Springer), and *Optical Switching and Networking* (Elsevier).